Xiangchun Xuan

Department of Mechanical Engineering,
Clemson University,
Clemson, SC, USA

Received April 20, 2007
Revised May 21, 2007
Accepted May 21, 2007

Review

Joule heating in electrokinetic flow

Electrokinetic flow is an efficient means to manipulate liquids and samples in lab-on-a-chip devices. It has a number of significant advantages over conventional pressure-driven flow. However, there exists inevitable Joule heating in electrokinetic flow, which is known to cause temperature variations in liquids and draw disturbances to electric, flow and concentration fields *via* temperature-dependent material properties. Therefore, both the throughput and the resolution of analytic studies performed in microfluidic devices are affected. This article reviews the recent progress on the topic of Joule heating and its effect in electrokinetic flow, particularly the theoretical and experimental accomplishments from the aspects of fluid mechanics and heat/mass transfer. The primary focus is placed on the temperature-induced flow variations and the accompanying phenomena at the whole channel or chip level.

Keywords:
Electrokinetic flow / Electroosmosis / Joule heating / Temperature
DOI 10.1002/elps.200700302

1 Introduction

Lab-on-a-chip devices have found wide applications in the analysis of chemical and biological samples. These integrated microfluidic devices offer many advantages over conventional bench-top analytical instruments, such as increased efficiency, throughput, and portability while reduced analysis time, reagent consumption, and cost [1–10]. An efficient technique for manipulating liquids and samples in these chip-based microfluidic systems is electrokinetic flow [11, 12]. This flow transports liquids by electroosmosis and samples (*e.g.*, ions, particles, and cells) by electrophoresis, both of which are generated through the interaction of an applied electric field and the electric double layer (EDL) at the solid–liquid interface [13, 14]. Therefore, pumps, valves, and other mechanical moving parts are eliminated in electrokinetic flow. More importantly, electrokinetic flow possesses a nearly plug-like velocity profile, causing reduced sample dispersion and enhanced flow conductance with respect to the traditional pressure-driven flow [15, 16].

Correspondence: Professor Xiangchun Xuan, Department of Mechanical Engineering, Clemson University, Clemson, SC 29634, USA
E-mail: xcxuan@clemson.edu
Fax: +1-864-656-7299

Abbreviations: EDL, electric double layer; **μPIV,** microparticle-image velocimetry technique; **TGF,** temperature gradient focusing

However, there exists inevitable Joule heating in the liquid when an electric field is applied to generate electrokinetic flow through a microchannel [17, 18]. This internal heat source may lead to significant increase and nonuniformity in the liquid temperature [19, 20]. The elevated temperature, on one hand, may denature live biological samples [21], while on the other, may be exploited in heat related physico-chemical processes [22]. Meanwhile, as most liquid properties vary with temperature, the induced temperature gradients make the liquid properties nonuniform. Hence, disturbances are drawn to electrokinetic flow, causing significant deviations from its plug-like velocity profile. These variations reduce both the throughput and the resolution of analytic studies performed in lab-on-a-chip devices [11, 23]. Therefore, it is important to study Joule heating and its effect on the electrokinetic transport of liquids and samples in order for the optimal design and efficient operation of microfluidic systems.

This article attempts to review the topic on Joule heating in electrokinetic flow. We focus primarily on the recent progress in theoretical and experimental studies of temperature-induced flow variations and the accompanying phenomena at the whole channel or chip level. In general, the theoretical and experimental approaches involved in this article are only briefly mentioned. For a comprehensive knowledge of these methods, readers are referred to Erickson [24] for a review of numerical modeling of integrated microfluidic devices, to Xuan and Li [25] for a review of theoretical (analytical) models of Joule heating in electrokinetic flow, to Ross *et al.* [26] and Xuan [20] for a review of temperature measurement in microchannels, and to Sinton [27] for a review of microscale

flow visualization. Readers are also suggested to read Rathore's [28] review of Joule heating and temperature determination inside an open or packed capillary in capillary electrophoresis and electrochromatography. This article is written assuming readers have at least a rudimentary understanding of electrokinetic phenomena, which are well documented in classical reference texts on electrokinetics such as Hunter [13], Lyklema [14], Li [16], and Masliyah [29].

2 Temperature-dependent material properties

Prior to discussing Joule heating and its effect on electrokinetic flow in microchannels, a brief overview of the temperature dependence of the involved material (including liquid, sample, and channel wall) properties is warranted. For the liquid properties, we focus mainly on aqueous solutions. Nevertheless, background electrolytes prepared in organic solvents, *i.e.*, nonaqueous solutions, have also found many applications in capillary electrophoresis due to a number of advantages compared to aqueous solutions [30–35]. One such advantage states that the lower electric current (and thus a lower Joule heating) in nonaqueous solutions should theoretically enable a higher separation voltage and therefore a shorter analysis time. This statement is, however, not generally true in organic solvent systems. Readers interested in the topic of Joule heating in nonaqueous solutions are referred to a recent critical review by Porras and Kenndler [36].

It is more convenient to divide the material properties into the following three categories: heat transfer-related, liquid (or more precisely, momentum) transfer-related, and mass transfer-related. Among the first category, electric conductivity of the background electrolyte solution is the direct property dictating the extent of Joule heating. The vast majority of previous studies assumed that electric conductivity λ is a linear function of liquid temperature T (in unit of K), *i.e.*, $\lambda = \lambda_0[1 + \alpha(T - T_0)]$ [37–40], where λ_0 is the conductivity at the reference temperature (or simply the room temperature) T_0 and α is the temperature coefficient. However, if the temperature variation $(T - T_0)$ gets large, adding a quadratic-dependence term would give more accurate results, as demonstrated by Porras and co-workers [33]. It is also noted that λ_0 is frequently assumed proportional to the ionic concentration unless the electrolyte solute is concentrated [38–40]. The other two properties within the first category are thermal conductivity and heat capacity, which can be safely assumed constant in most cases [41].

Among the second category, wall zeta potential ζ, liquid viscosity η, and liquid permittivity ε are equally important in the Helmholtz–Smoluchowski velocity (*i.e.*, electroosmotic slip velocity), $u_{HS} = -\varepsilon\zeta E/\eta$ [13, 14, 16, 29]. For dilute aqueous solutions, their viscosity and permittivity are roughly the same as those of pure water, which may be expressed as, for example, $\eta = 2.761 \times 10^{-3} \exp(1713/T)$ (in unit of $kgm^{-1}s^{-1}$) and $\varepsilon = 305.7 \exp(-T/219)\varepsilon_0$ (in unit of $CV^{-1}m^{-1}$, ε_0 is the vacuum permittivity) [42, 43]. The temperature dependence of zeta potential is generally complex and hard to be isolated from other properties for quantification. However, two recent experiments both demonstrated a linear temperature function of zeta potential though its slope may vary significantly with respect to the choice of solution and substrate [44, 45]. For example, Venditti *et al.* [45] presented in Table 1 the measured zeta potential values for a number of commonly used buffers. Their results show that in some solutions (*e.g.* KCl, Tris-borate-EDTA (TBE)) the zeta potential increases significantly with temperature, while other buffers (*e.g.* TE, $Na_2CO_3/NaHCO_3$) seem to be stable over all measured temperatures. For more information on zeta potential of microfluidic substrates, readers are referred to Kirby and Hasselbrink [46, 47].

Among the third category, diffusion coefficient D of samples may vary by a few orders of magnitude depending on their size. However, it is usually a good approximation to use the Stokes–Einstein relation for the determination of D, that is, $D = k_B T/6\pi\eta a$, where k_B is Boltzmann's constant and a is the radius of sample molecules [14, 29]. As discussed earlier, viscosity η is known to decrease with the rise of liquid temperature T, so the molecular diffusion exhibits a strong positive dependence on T. Another material property falling into this category is the ionic mobility of sample species,

Table 1. Summary of measured zeta potential results

Solution	Concentration	ζ (30°C) (mV)	$\zeta = \zeta(T)$ (mV, °C)
KCl	0.1 mM	−108.2	$-0.06T - 107.4$
	1 mM	−92.6	$-0.44T - 78.2$
		(−78.2)	$(-0.20T - 72.8)$
	10 mM	−56.4	$-0.48T - 43.8$
		(−38.4)	$(-0.09T - 35.5)$
$Na_2CO_3/NaHCO_3$	10 mM	−92.9	$+0.02T - 93.1$
1 × TE	10 mM Tris, 1 mM EDTA	−68.2	$-0.01T - 67.9$
1 × TBE	89 mM Tris, 89 mM boric acid, 2 mM EDTA	−52.4	$-0.35T - 40.0$

Bracketed entries denote PDMS:PDMS microchannels. All other entries represent PDMS:glass. Adapted from ref. [45].

ν, which is closely related to its electric conductivity (note: not the conductivity λ of the background electrolyte) [14]. Nernst–Einstein relation, $\nu = D/RT$ with the universal gas constant R, is often used to relate ionic mobility to its diffusion coefficient [29]. As such, $\nu = 1/6\pi\eta a N_A$, where N_A is the Avogadro constant, is an inverse function of liquid viscosity and hence increases with temperature.

3 Joule heating in electrokinetic microchannel flows

From this section on, we review the recent progress in the topic of Joule heating and its effect on electrokinetic flow in single microchannels (Section 3) and microchannel systems (Section 4), respectively. The former circumstance is mostly relevant to capillary electrophoresis and electrochromatography as well as electroosmotic pumping. Those on Joule heating effects in microchannel systems are stipulated by the rapidly growing applications of polymeric microfluidic chips, whose base materials, for example, poly(dimethylsiloxane) (PDMS), generally have a low thermal conductivity [48].

The vast majority of previous work on Joule heating in electrokinetic microchannel flows concerns only the lateral (or radial in a round capillary) temperature variations by assuming an infinitely long tube with its outer surface subject to a uniform heat transfer condition. In real flow systems, however, there exist at least two factors that may cause axial temperature gradients: one is the reservoir-based cooling effects because electroosmosis keeps pulling the cool liquid from the inlet reservoir while pushing the hot liquid into the outlet reservoir, which is named as thermal end effects by Xuan *et al.* [49]; the other is the nonuniform dissipation of Joule heating along the channel length direction, which might be the consequence of variable cooling conditions [50, 51], nonuniform channel cross-section [26, 52, 53], or discontinuous electric conductivity of the sample with respect to the background electrolyte in the case of, for example, sample stacking and pumping [54, 55]. Below we start with the review of the work on lateral temperature gradients in single microchannels. Immediately following is the discussion of axial temperature gradients due to thermal end effects and nonuniform cooling, respectively. Other topics of interest that are pertinent to Joule heating in electrokinetic microchannel flows are also presented.

3.1 Lateral temperature gradients

Joule heating has been long known to cause an increase and a radial nonuniformity in liquid temperature in capillary electrophoresis [17, 42, 56]. As a number of previous reviews have partially covered this issue, for example, Gaš *et al.* [17], Ghosal [18], and Rathore [28], we here only briefly mention the contributions from various authors. By assuming a constant liquid conductivity, Knox [43], Knox and McCormack [57, 58], and Grushka *et al.* [59] obtained a parabolic temperature profile over the channel cross-section. However, Gobbie and Ivory [60] later pointed out that assuming a constant electric conductivity resulted in underestimated liquid temperatures because in reality, conductivity increases with temperature as noted above. Moreover, the phenomenon of thermal runaway is missed under this assumption. Employing a linear relationship to describe the temperature dependence of liquid conductivity, Jones and Grushka [38], and Bello and Righetti [39, 40] studied the steady state and transient state liquid temperatures, and both demonstrated an essentially parabolic temperature profile over the capillary cross-section. With these lateral temperature variations, however, the profile of electroosmotic velocity still remains plug-like in the bulk region despite the increased magnitude due to the drop of liquid viscosity [18]. All velocity gradients are restricted to within the thin EDL (on the order of nanometer). Meanwhile, both electrophoretic velocity and molecular diffusion of analyte species become nonuniform over the channel cross-section, causing the so-called Taylor dispersion. For the origin and theoretical foundation of such dispersion, readers are referred to Taylor [61] and Aris [62].

The problem of dispersion caused by the Joule heating-induced parabolic profile of electrophoretic velocity has been examined both theoretically and experimentally. Knox and Grant [43, 57, 58] and Grushka *et al.* [59] derived an analytical formula to account for this effect on the theoretical plate height in capillary electrophoresis. Gobbie and Ivory [60] suggested using an opposing Poiseuille flow to counter for the thermally parabolic distortion of the migration velocity. They also derived a formula for the resulting plate height based on the Taylor–Aris dispersion theory. Andreev and Lisin [63, 64] numerically calculated the peak broadening due to the nonuniform liquid electroosmosis, species electrophoresis and diffusion. Such coupled contribution was recently included in Xuan and Li's [65] analytical model which is essentially applicable to capillary columns of arbitrary size and zeta potential. More recently, Peterson *et al.* [66] compared Joule heating effects in microchip-based and capillary-based electrophoretic separation systems. They concluded that the influence of Joule heating on separation efficiency is mainly associated with the radial profile rather than the overall rise in liquid temperature. This judgment seems, however, inconsistent with some previous experiments [33, 34], which was later explained by Xuan and Li [67] using the axial temperature gradients-induced pressure-driven flows and will be addressed shortly. For details of dispersion in electrokinetic flow due to other sources of band broadening, readers may be referred to Gaš *et al.* [17, 68, 69] and Ghosal [18, 23].

3.2 Axial temperature gradients due to thermal end effects

Tang *et al.* first numerically investigated the effect of Joule heating on liquid electroosmotic flow and species transport in cylindrical [70] and slit [71] microchannels. Thermal end

effects were found to produce both lateral and axial temperature gradients in the liquid. Assuming a uniform electric field along the whole channel, they predicted an enhanced liquid flow with a convex profile in the developing region while concave in the fully developed region. These deviations from the plug-like profile of electroosmotic velocity are attributed to the thermally induced pressure-driven flows. Such nonuniform temperature and velocity fields then make the sample front translate faster but more dispersed. The same authors later validated the applicability of Poisson–Boltzmann equation in describing the ionic distribution through comparison to the full Nernst–Planck equation [72].

Other than the momentum and mass transport, however, the axially nonuniform temperature distribution should also affect the charge transport because of the resultant nonuniformity in liquid conductivity. This issue was first addressed by Xuan *et al.* [49] in a whole-capillary (from reservoir to reservoir) simulation. They proposed that the electric field strength must be also nonuniform along the length direction in order to satisfy the condition of current continuity. Specifically, the electric field strength close to the capillary ends is much higher than in the middle part because the liquid conductivity in the former region is lower due to thermal end effects. Consequently, the electric body force is greater close to the channel ends, leading to a locally higher electroosmotic velocity (see, for example, the Helmholtz–Smoluchowski velocity, $u_{HS} = -\varepsilon\zeta E/\eta$) [13, 14, 16, 29]. Then, the condition of mass continuity gives rise to an asymmetrically sine-shaped distribution of pressure along the channel length direction. Therefore, the radial profile of liquid velocity is expected to be concave near the inlet and the outlet while slightly convex in the middle of the capillary.

Xuan *et al.* [73] later verified their numerical predictions of both the axial temperature distribution and the radial velocity profile in the liquid using fluorescence-based microscale visualization techniques. They measured the liquid temperature at a series of points inside a bare capillary by monitoring the variation of fluorescence intensity emitted from temperature-dependent rhodamine B dye. As seen in Fig. 1, sharp temperature drops arise close to both the inlet and outlet of the capillary due to thermal end effects while in its main body a high-temperature plateau is shifted to the downstream due to the advective flow effect. The higher the electric field (and thus the larger electroosmotic velocity) is, the more significant the inclination becomes. These predictions are in good agreement with their whole-capillary simulation [49].

The liquid velocity in electrokinetic microchannel flows was obtained by visualizing the electrokinetic transport of uncaged fluorescent dye. The predicted concave and convex velocity profiles were observed in different regions of a capillary. However, the measured profiles were more significantly curved than those from the numerical simulation, particularly in the middle region at high electric fields. In the same experiment the measured average liquid velocities, however, agreed well with their numerical predictions at

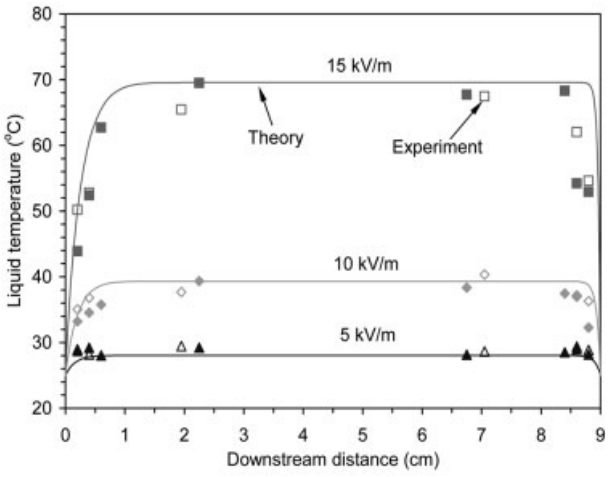

Figure 1. Comparison between numerically (solid lines) and experimentally (markers) obtained temperature distributions along the capillary axis 15 s after the indicated electric fields were applied. Hollow and filled markers represent measurements in different days. Adapted from ref. [73].

both transient and steady states. For details of the numerical simulation and flow visualization, readers are referred to Xuan *et al.* [73]. More recently, Tang *et al.* [74] used the microparticle-image velocimetry technique (μPIV) to study the influence of Joule heating on the profile of electroosmotic velocity in a rectangular microchannel fabricated in PDMS. As demonstrated in Fig. 2, these authors obtained a concave (Fig. 2a) and a convex (Fig. 2b) flow profile close to the inlet and middle of the microchannel, which agreed well with their 3-D numerical simulation. Johnson *et al.* [75] also saw a slightly convex velocity profile in a straight microchannel. These observations further demonstrate the existence of thermal end effects in electrokinetic microchannel flows as discussed earlier.

As a consequence of the increased magnitude and the curved profile of liquid velocity, the electrokinetic migration of discrete sample zone is sped up while subject to extra Taylor dispersion. This thermally originated dispersion is mainly attributed to the induced pressure-driven liquid flow, which is distinctly different from the previously addressed thermal dispersion associated with the parabolic profile of species electrophoretic velocity [17, 18, 23]. Xuan and Li [76] developed an analytical model to address Joule heating effects on the transport of heat, electricity, momentum, and mass species in capillary electrophoresis. Compact formulae were proposed for predicting the enhancing effect of Joule heating on both electric current and throughput (*i.e.*, flow rate) in the presence of thermal end effects. However, these authors admitted that their analytical model applied only to cases with not-too-strong electric field due to the linear assumption made in their derivation. This restriction was recently released in Chein *et al.*'s [77] analytical model that predicted in good accuracy the experimentally measured

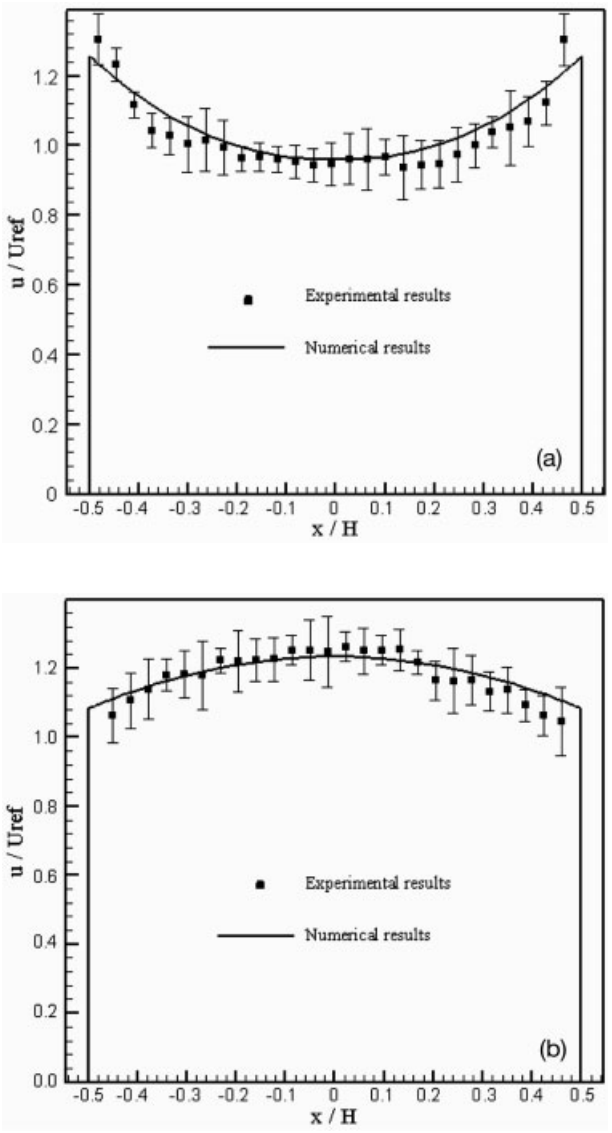

Figure 2. Comparison of electroosmotic flow velocity distribution along the transverse direction between μPIV experimental results and numerical predictions for electrokinetic flow with Joule heating effects in (a) entry region and (b) downstream region of a PDMS:glass microchannel. Adapted from ref. [74].

temperatures. Their model, however, failed to predict properly the flow field because a uniform electric field had been assumed throughout the channel.

Xuan and Li [76] also derived a close-form formula for the electrokinetic migration of sample zone in capillary electrophoresis. Their formula reveals that the sample zone migrates through the detector in a shorter time period (advantage) while at a broader peak width (and thus a lower peak height, disadvantage). These influences are both apparent in Fig. 3, which compares the concentration profiles of a sample zone at different time instants with and without consideration of Joule heating effects. Similar

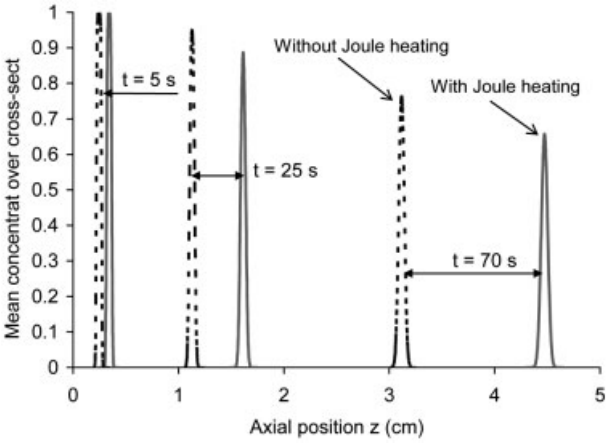

Figure 3. Mean concentration of a sample zone over the capillary cross-section at different times. The solid lines indicate the distributions along the capillary with consideration of Joule heating effects whiles those dashed lines are without Joule heating effects. In both cases, the sample zone initially has a width of five times the capillary internal radius and a unit concentration. Adapted from ref. [76].

findings were also reported in Tang *et al.*'s [74, 78, 79] numerical simulations, where the second order Crank–Nicolson scheme was employed to minimize the numerical diffusion. Hence, an optimum condition or a tradeoff between analysis time and species peak width might exist, which certainly deserves further studies.

3.3 Axial temperature gradients due to nonuniform cooling

By inserting the middle part of a capillary into a cooling water-bath while remaining the rest parts in the air, Gaš [50] studied the influence of nonuniform cooling on species electrophoretic separation. Such variations of heat transfer condition along the length direction often exist in capillary electrophoresis with thermostating, where a short length of the capillary at each end must be left outside the thermostated cartridge for sample injection and detection. Since these two regions are normally exposed to free air (*i.e.*, unthermostated), the local liquid temperature is higher than that in the middle region with forced-air (or liquid) cooling. In other words, axial temperature gradients are induced passively by the nonuniform dissipation of Joule heating. Then, as we discussed earlier, the condition of current continuity requires that the electric field strength in the thermostated region be higher than the rest, and the condition of mass continuity forces the appearance of axial pressure gradients causing different disturbances to the electroosmotic flow field.

Xuan and Li [67] developed an analytical model to predict the band broadening in capillary electrophoresis with axially nonuniform cooling in terms of the theoretical plate height.

By considering the continuity conditions of electric current and flow rate through a capillary, they derived formulae for the liquid temperature, electric field strength, liquid velocity, sample velocity, and dispersion in each individual region as referred to above. These authors demonstrated in Fig. 4 that the plate height due to axial temperature gradients (H_{axT}, refer to the left ordinate, in unit of μm) may be one order of magnitude larger than that due to the radial temperature gradients (H_{radT}, refer to the right ordinate, in unit of nm), and even comparable to that due to species diffusion (H_{dif}, refer to the left ordinate). This model has been used to explain the phenomena observed in Palonen's experiments [33, 34]. Moreover, the prediction of a concave velocity profile in the thermostated region is supported by Sinton *et al.*'s experiment [51], where a drop of immersion oil surrounding a short length capillary of the middle section acted as the thermostating cartridge. Figure 5a shows the image sequence of uncaged fluorescent dye transport in the oil viewing window, and Fig. 5b shows the temporal development of the velocity profile with profiles obtained at different times after the application of the electric field. Note that the $t = 20$ s case corresponds to the image sequence.

Recently, Palonen *et al.* [35] observed higher separation efficiency in nonaqueous electrophoretic separation with an initial voltage ramp, which was stated to be of thermal origin. Xuan *et al.* [80] later theoretically verified this statement in some sense. By considering the temporal and spatial variations of the nonuniform temperature and flow fields, these authors demonstrated that the application of an initial voltage ramp delays the development of Joule heating-induced pressure-driven flows. The thermal dispersion is thus significantly reduced resulting in the enhanced separation efficiency. This enhancement is, however, only apparent in noncoated capillaries, which is consistent with the reported

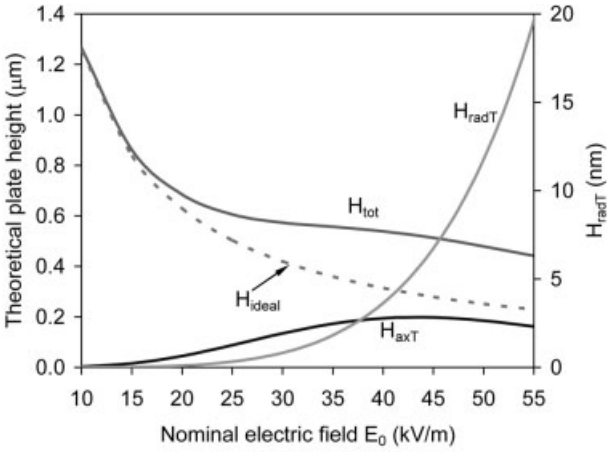

Figure 4. Theoretical plate heights at different electric fields. H_{tot} indicates the total plate height including the contribution from molecular diffusion and Joule heating. H_{ideal} indicates the minimum plate height in capillary electrophoresis where diffusion is the only source of band broadening. Note that only H_{radT} refers to the secondary *Y*-axis (*i.e.*, right ordinate). Adapted from ref. [67].

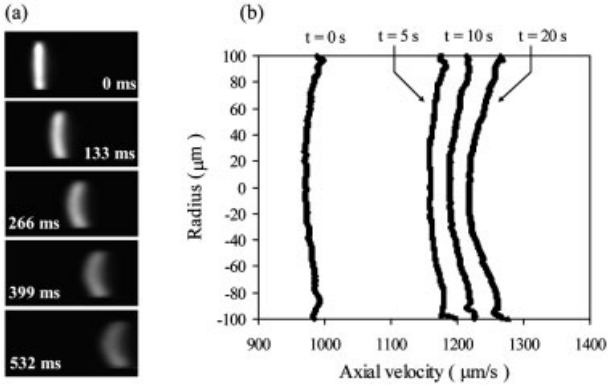

Figure 5. Electrokinetic flow in a 200 μm id circular capillary at an electric field of 15 kV/m: (a) image sequence of uncaged fluorescent dye transport with image timing inset. (b) Temporal development of the velocity profile is shown with profiles obtained at $t = 0$, 5, 10, and 20 s after the application of the electric field (the $t = 20$ s case corresponds to the image sequence). Adapted from ref. [51].

measurements in both aqueous and nonaqueous capillary electrophoresis [81–83]. In coated capillaries where the electroosmotic flow is suppressed, however, an opposite trend was actually predicted. This issue may deserve further studies.

3.4 Other topics of interest

There have also appeared some other interesting topics related to Joule heating in electrokinetic microchannel flows. Zhao and Liao [84] numerically studied the effect of Joule heating on the electroosmotic pumping of liquids between two parallel plates. By assuming isothermal conditions on the two plates, they predicted a much lower pressure head than that free of Joule heating. Maynes and Webb [85] theoretically analyzed the fully developed electroosmotic heat transfer in slit and circular microchannels under constant wall heat flux and constant wall temperature boundary conditions. They found that the Nusselt number in electroosmotic flow is dependent on both the magnitude of Joule heating and the relative channel size (*i.e.*, ratio of channel width to EDL thickness). Later, their analytical model was extended by Horiuchi and Dutta [86] to consider the thermally developing behavior of electroosmotic flows in two-dimensional microchannels. In the range of low Reynolds number ($Re \leq 0.7$), the Nusselt number was found independent of the thermal Peclet number except in the thermally developing region.

Rathore *et al.* [87] experimentally investigated the Joule heating in packed capillaries for the use in capillary electrochromatography by monitoring the electric current at variable applied voltages. Based on the fact that Joule heating increases the electric conductivity of a liquid due to its temperature dependence, heat dissipation was found to be

not always efficient under typical mobile and stationary phase conditions. Similar findings were also reported in Chen *et al.*'s [88] work. Kang *et al.* [89] presented a numerical modeling of Joule heating effects on the transient temperature field and electroosmotic flow field in a microcapillary packed with microspheres. Similar to Xuan *et al.*'s [49, 73] and Tang *et al.*'s [74, 79] analyses in capillary electrophoresis (open channel, free column), noticeable axial temperature gradients occur in the thermal entrance region, and axial pressure gradients are induced to maintain the mass continuity.

Also of interest is the effect of Joule heating on the stability of time-modulated electroosmotic flow. Through a theoretical analysis, Chang and Homsy [90] concluded that Joule heating generally acts to stabilize the liquid flow. In addition, Wang *et al.* [91] examined analytically the effect of Joule heating on sample dispersion in electrophoretic separation microchannels. These authors stated that their model could be used to determine the analyte dispersion in microchannels of general shapes, for instance, serpentine- or spiral-shaped channels. Recently, Evenhuis *et al.* [92] used the conductance measurement to perform a systematic comparison of internal electrolyte temperatures among fused-silica and a few other polymer capillaries. They found that the average increase in the mean liquid temperature is inversely proportional to the thermal conductivity of each type of capillary material. They also proposed a novel method of determining the liquid temperature at the capillary wall by measuring the electroosmotic mobility [93]. This method in conjunction with the conductance measurement can give rise to the temperature profile across the capillary cross-section. More recently, Xuan [94] revisited Joule heating in capillary electrophoresis by considering the increased conductivity within EDL. He demonstrated that such contribution of the so-called surface conductance [95] is generally negligible in terms of the temperature profile.

4 Joule heating in electrokinetic microfluidic chips

Very little work has been done on Joule heating in electrokinetic flow that takes place in microfluidic chips. It is mainly due to the simultaneous presence of four separate length scales: the chip size of centimeters, the channel length of millimeters, the channel cross-sectional dimension of micrometers, and the EDL thickness of nanometers. Therefore, in the theoretical aspect, a full solution of the temperature (extend to the whole chip due to thermal diffusion) and flow (only in the fluid region) fields on all the four length scales would require a prohibitive amount of memory and computational time. In the experimental aspect, a novel technique would have to be developed to measure the whole chip temperature at a resolution of at least the same order of channel cross-sectional dimension (*i.e.*, micrometers).

Erickson *et al.* [96] first studied Joule heating in electrokinetic microfluidic chips. They used a combined experimental (a microscale thermometry technique) and numerical (a 3-D "whole-chip" finite element method) approach to examine Joule heating and heat transfer at a T-shaped microchannel intersection in PDMS:PDMS and PDMS:glass microfluidic systems. At high electric field strengths, they observed a nearly five-fold increase in the maximum liquid temperature in the PDMS:PDMS chip over the PDMS:glass chip. Figure 6 shows the comparison between numerically and experimentally obtained temperature profiles for the aforementioned two chips. These authors have also reported a number of significant secondary effects of Joule heating including the increased current load and the enhanced flow rate.

Lim *et al.* [97] presented a theoretical study of the effect of channel topologies on electrophoretic separations. They demonstrated that topological patterns, such as finned structures, can dramatically enhance a channel's ability to dissipate Joule heating and as well reduce the axial dispersion associated with the siphoning effect. This improvement is especially beneficial to situations requiring large volumetric throughput, for example, in preparative or semi-

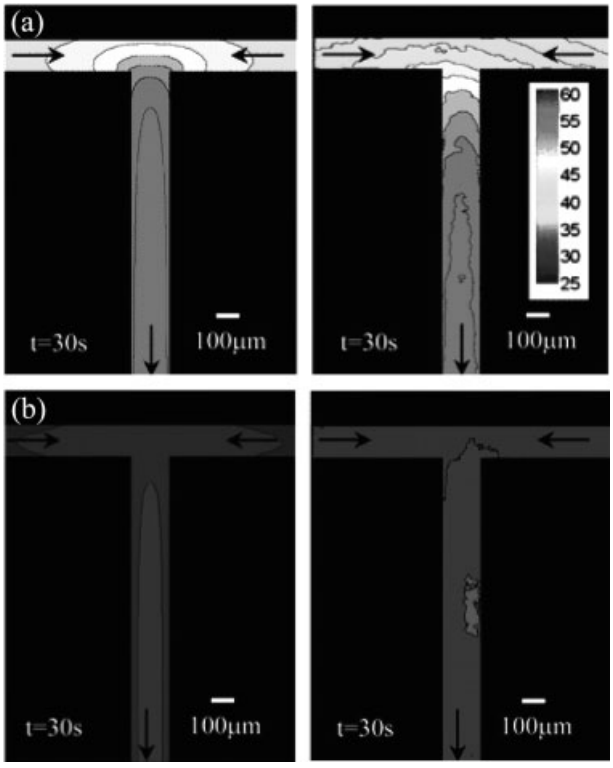

Figure 6. Comparison between numerically (left column) and experimentally (right column) obtained temperature profiles in a T intersection for (a) PDMS:PDMS and (b) PDMS:glass microfluidic chips, respectively. In each case, a 2.05 kV electric field was applied to the inlet reservoirs while the outlet reservoir was grounded, corresponding to an average electric field strength of 137 kV/m. Adapted from ref. [96].

preparative scale operations. Recently, Huang and Yang [98] investigated the effect of Joule heating on electrokinetic focusing using a 2-D numerical simulation. It was found that Joule heating causes two influences on the focusing ratio: one is the enhanced thermal diffusion which broadens the focused width, and the other is the induced nonuniform flow field which may tighten or broaden the focused width depending on the locally concave or convex flow profile.

5 Applications of Joule heating in electrokinetic microfluidic devices

As discussed above, the major concern of Joule heating in electrokinetic flow continues to be how to minimize the temperature effects in microfluidic devices. In other words, Joule heating is mostly viewed as a disadvantage to electrokinetic flow. In this section, however, we provide a brief overview of some of the recent applications of Joule heating in electrokinetically driven microfluidic devices, *i.e.*, the advantage of Joule heating.

De Mello *et al.* [22] proposed the use of Joule heating of ionic liquids as an effective method of controlling temperatures with high precision and accuracy within microchannel environments. The ionic liquid held in a corunning channel was Joule heated with an AC current, and its temperature could be extracted from the measured conductivity *via* the known temperature function without need of on-chip thermocouples. These authors demonstrated that temperatures can be maintained to within ± 0.2°C. A similar method to control polymerase chain reaction (PCR) thermal cycling was recently presented by Hu *et al.* [99], where the denaturation (94°C) and annealing/extension (63°C) temperatures for the amplification of *E. coli* DNA were controlled by adjusting the electric current through the PCR solution. The switch between high and low currents and the dwelling at each current level was implemented by a high-voltage sequencer that had been programmed based on their numerical simulation. Such a PCR PDMS chip required only a 1.3 W power input.

As mentioned earlier, axial temperature gradients are set up in a channel with variable cross-sections due to nonuniform Joule heating. These temperature gradients can create pH gradients when a proper medium is used, which holds the potential for isoelectric focusing applications. Pawliszyn and coworkers [100, 101] accomplished such focusing applications by utilizing nonuniform Joule heating along the axis of first a tapered capillary and later a tapered plastic microchannel sandwiched between two glass slides [102]. In the latter case, the thermally generated pH gradient separation of proteins was demonstrated by focusing dog, cat, and human hemoglobins in Tris-HCl buffer that has a high pK_a dependence of temperature. More recently, Kates and Ren [53] developed a 3-D numerical model to study the Joule heating and heat transfer in a microfluidic chip with a diverging microchannel. It was found that the channel geometry has significant effects on the peak temperature location, while the medium conductivity and the chip surface convection influence the temperature gradients and thus the resultant pH gradients. Their simulation also reveals the significance of liquid flow effect on temperature distribution.

The nonuniform Joule heating in a channel with variable cross-sections has also been used to realize the so-called temperature gradient focusing (TGF) [52, 103, 104]. Ross and Locascio [52] first demonstrated the TGF at a junction of two microchannels of different cross-sectional area using an 8 μM Oregon Green 488 carboxylic acid. At an applied voltage of 1900 V, they achieved a temperature gradient spanned from 23 to 39°C with a maximum gradient of 150°C/mm, with which a greater than 300-fold increase in concentration was observed within 190 s. Based on the same principle, Kim *et al.* [105] recently developed a simple variable-width PDMS device, which could deliver rapid and repeatable electrokinetic focusing of model analytes using significantly lower power than conventional TGF methods [103, 104]. This microfluidic chip implemented simultaneous separation and concentration of a mixture of 25 μM fluorescein-Na and 100 nM fluorescein isothiocyanate conjugate bovine serum albumin (FITC-BSA) in 900 mM Tris-borate buffer in less than 10 min.

Another topic of interest is the electrothermally induced fluid flow that was recently exploited by Sigurdson *et al.* [106] to enhance microfluidic immunosensors, for example, immunoassays, by microstirring analyte near the functionalized binding surface. Such flow is generated by the electrothermal force [107, 108] which stems from the interactions between the nonuniform electric field close to an electrode and the Joule heating-induced nonuniformities in liquid conductivity and permittivity. Due to the normally circulating pattern of electrothermally induced fluid flow [109], see Fig. 7c, the binding rate of antigen to immobilized ligands is predicted in Sigurdson *et al.*'s simulation to increase by a factor of 7 compared to the case with pressure-driven flow at the optimized conditions. Figure 7 demonstrates the concentration plots of electrothermally modified channel flow with a voltage of (a) 0 Vrms (*i.e.*, pressure-driven flow) and (b) 6 Vrms applied to the indicated electrodes. The influence of the electrothermally induced pair of counter rotating vortices on the concentration profile is apparent, see in Fig. 7c the fluid velocity adjacent to the two electrodes obtained from μPIV.

6 Concluding remarks and outlook

As discussed above, the majority of the work reported so far on Joule heating in electrokinetic flow concerns only the fundamental research, *e.g.*, its effect on the flow profile of liquid and the dispersion of sample species. Very little work has been conducted on the applied research, *e.g.*, can Joule heating be used for the fine manipulation of liquid motion and species transport? Therefore, future directions for research may be focused on the application of Joule heating in

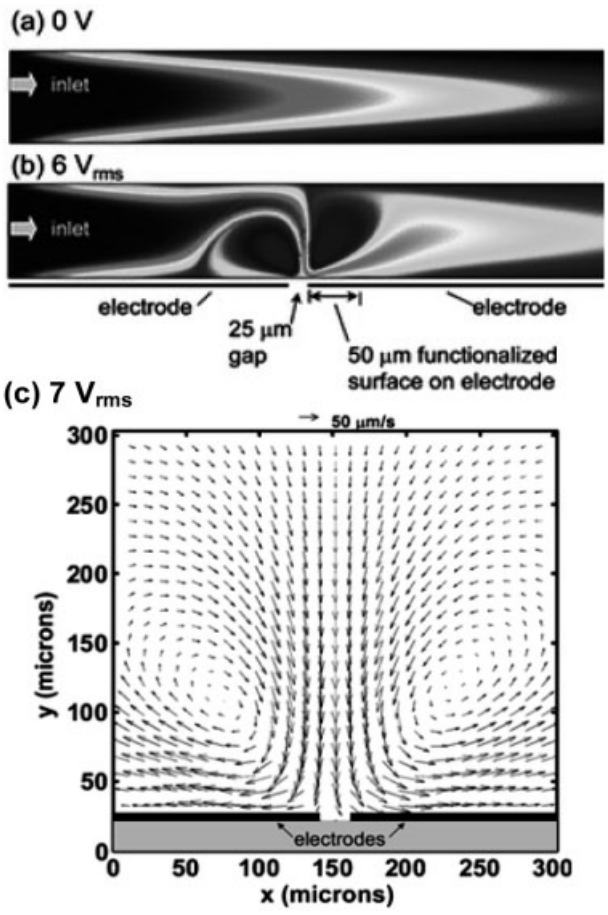

Figure 7. Concentration plots of electrothermally modified channel flow with applied voltages of (a) 0 and (b) 6 Vrms; (c) shows the zoom-in fluid velocity field adjacent to the two working electrodes indicated in (b), which was obtained from μPIV at an applied voltage of 7 Vrms. Adapted from ref. [107].

electrokinetic microfluidic devices. Some specific examples may include but not necessarily restricted to: Joule heating-induced axial temperature gradients for concentrating and separating macromolecules (other than the TGF and isoelectric focusing), for example, DNA; Joule heating-induced lateral temperature gradients for optical waveguiding [110]; Joule heating assisted micromixing, *etc*. As to the future directions for fundamental research, it may be interesting and also important to examine the role of Joule heating in electrokinetic instability with conductivity gradients [111], to quantify the effect of Joule heating on sample stacking/pumping with discontinuous conductivity, to determine the appropriate thermal boundary conditions in a microfluidic chip, and to develop a numerical method for the efficient simulation of Joule heating at a whole chip level.

Financial support from Clemson University through a start-up package to Xuan is gratefully acknowledged.

The authors declare no conflict of interest.

7 References

[1] Stone, H. A., Kim, S., *AIChE J.* 2001, *47*, 1250–1254.

[2] Reyes, D. R., Iossifidis, D., Aurous, P., Manz, A., *Anal. Chem.* 2002, *74*, 2623–2636.

[3] Aurous, P., Iossifidis, D., Reyes, D. R., Manz, A., *Anal. Chem.* 2002, *74*, 2637–2652.

[4] Selvaganapathy, P. R., Carlen, E. T., Mastrangelo, C. H., *Proc. IEEE* 2003, *91*, 954–975.

[5] Hansen, C., Quake, S. R., *Curr. Opin. Struct. Biol.* 2003, *13*, 538–544.

[6] Erickson, D., Li, D., *Anal. Chim. Acta* 2004, *57*, 11–26.

[7] Tegenfeldt, J. O., Prinz, C., Cao, H., Huang, R. L. *et al.*, *Anal. Bioanal. Chem.* 2004, *378*, 1678–1692.

[8] Pihl, J., Karlsson, M., Chiu, D. T., *Drug Discov. Today* 2005, *10*, 1377–1383.

[9] Toner, M., Irimia, D., *Annu. Rev. Biomed. Eng.* 2005, *7*, 77–103.

[10] See, for example, a special issue in *Nature* dedicated to Lab-on-a-chip: *Nature*, 2006, *442*, 367–418.

[11] Stone, H. A., Stroock, A. D., Ajdari, A., *Annu. Rev. Fluid Mech.* 2004, *36*, 381–411.

[12] Squires, T. M., Quake, S. R., *Rev. Modern Phys.* 2005, *7*, 977–1026.

[13] Hunter, R. J., *Zeta Potential in Colloid Science, Principals and Applications*, Academic Press, New York 1981.

[14] Lyklema, J., *Fundamentals of Interface and Colloid Science*, Academic Press, New York 1995, Vol.II.

[15] Whitesides, G. M., Stroock, A. D., *Phys. Today* 2001, *54*, 42–48.

[16] Li, D., *Electrokinetics in Microfluidics*, Elsevier Academic Press, Burlington, MA 2004.

[17] Gaš, B., Štědrý, M., Kenndler, E., *Electrophoresis* 1997, *18*, 2123–2133.

[18] Ghosal, S., *Electrophoresis* 2004, *25*, 214–228.

[19] Palonen, S., *Ph. D. Thesis*, Helsinki University Publishing House, Helsinki 2005.

[20] Xuan, X., *Ph. D. Thesis*, University of Toronto, Toronto, Canada 2006.

[21] Lindquist, S., *Annu. Rev. Biochem.* 1986, *55*, 1151–1191.

[22] De Mello, A. J., Habgood, M., Lancaster, N. L., Welton, T., Wootton, R. C. R., *Lab Chip* 2004, *4*, 417–419.

[23] Ghosal, S., *Annu. Rev. Fluid Mech.* 2006, *38*, 309–338.

[24] Erickson, D., *Microfluid. Nanofluid.* 2005, *1*, 301–318.

[25] Xuan, X., Li, D., in: Li, D. (Ed.), *Encyclopedia of Microfluidics and Nanofluidics*, Springer, Heidelberg, Germany 2007, in press.

[26] Ross, D., Gaitan, M., Locascio, L. E., *Anal. Chem.* 2001, *73*, 4117–4123.

[27] Sinton, D., *Microfluid. Nanofluid.* 2004, *1*, 2–21.

[28] Rathore, A. S., *J. Chromatogr. A* 2004, *1037*, 431–443.

[29] Masliyah, J. H., *Electrokinetic Transport Phenomena*, Alberta Department of Energy, Edmonton 1994.

[30] Palonen, S., Jussila, M., Porras, S. P., Hyotylainen, T., Riekkola, M., *J. Chromatogr. A* 2001, *916*, 89–99.

[31] Palonen, S., Jussila, M., Porras, S. P., Hyotylainen, T., Riekkola, M., *Electrophoresis* 2003, *23*, 393–399.

[32] Porras, S. P., Marziali, E., Gaš, B., Kenndler, E., *Electrophoresis* 2003, *24*, 1553–1564.

[33] Palonen, S., Jussila, M., Porras, S. P., Riekkola, M., *Electrophoresis* 2003, *24*, 1565–1576.

[34] Palonen, S., Jussila, M., Porras, S. P., Riekkola, M., *Electrophoresis* 2004, *25*, 344–354.

[35] Palonen, S., Jussila, M., Riekkola, M. L., *J. Chromatogr. A* 2005, *1068*, 107–114.

[36] Porras, S. P., Kenndler, E., *Electrophoresis* 2005, *26*, 3203–3220.

[37] Landers, J. P., *Handbook of Capillary Electrophoresis*, CRC, New York 1996.

[38] Jones, A. E., Grushka, E., *J. Chromatogr.* 1989, *466*, 219–225.

[39] Bello, M. S., Righetti, P. G., *J. Chromatogr.* 1992, *606*, 95–102.

[40] Bello, M. S., Righetti, P. G., *J. Chromatogr.* 1992, *606*, 103–111.

[41] Incropera, F. P., DeWitt, D. P., *Fundamentals of Heat and Mass Transfer*, Wiley, New York 1990.

[42] Knox, J. H., Grant, I. H., *Chromatographia* 1987, *24*, 135–143.

[43] Knox, J. H., *Chromatographia* 1988, *26*, 329–336.

[44] Evenhuis, C. J., Guijt, R. M., Macka, M., Marriott, P. J., Haddad, P. R., *Electrophoresis* 2006, *27*, 672–676.

[45] Venditti, R., Xuan, X., Li, D., *Microfluid. Nanofluid.* 2006, *2*, 493–499.

[46] Kirby, B. J., Hasselbrink, E. F., *Electrophoresis* 2004, *25*, 187–202.

[47] Kirby, B. J., Hasselbrink, E. F., *Electrophoresis* 2004, *25*, 203–214.

[48] Sun, Y., Kwok, Y. C., *Anal. Chim. Acta* 2006, *556*, 80–96.

[49] Xuan, X., Sinton, D., Li, D., *Int. J. Heat Mass Trans.* 2004, *47*, 3145–3157.

[50] Gaš, B., *J. Chromatogr.* 1993, *644*, 161–174.

[51] Sinton, D., Xuan, X., Li, D., *Exp. Fluid.* 2004, *37*, 872–882.

[52] Ross, D., Locascio, L. E., *Anal. Chem.* 2002, *74*, 2556–2564.

[53] Kates, B., Ren, C. L., *Electrophoresis* 2006, *27*, 1967–1976.

[54] Chien, R. L., *Electrophoresis*, 2003, *24*, 486–497.

[55] Sinton, D., Ren, L., Xuan, X., Li, D., *Lab Chip* 2003, *3*, 173–179.

[56] Hinckley, J. O. N., *J. Chromatogr.* 1975, *109*, 209–217.

[57] Knox, J. H., McCormack, K. A., *Chromatographia* 1994, *38*, 207–214.

[58] Knox, J. H., McCormack, K. A., *Chromatograhia* 1994, *38*, 215–221.

[59] Grushka, E., McCormick, R. M., Kirkland, J. J., *Anal. Chem.* 1989, *61*, 241–246.

[60] Gobbie, W. A., Ivory, C. F., *J. Chromatogr. A* 1990, *516*, 191–210.

[61] Taylor, G., *Proc. Roy. Soc. Lond. A* 1954, *219*, 186–203.

[62] Aris, R., *Proc. Roy. Soc. Lond. A* 1956, *235*, 67–77.

[63] Andreev, V. P., Lisin, E. E., *Electrophoresis* 1992, *13*, 832–837.

[64] Andreev, V. P., Lisin, E. E., *Chromatographia* 1993, *37*, 202–210.

[65] Xuan, X., Li, D., *J. Micromech. Microeng.* 2004, *14*, 1171–1180.

[66] Peterson, H. J., Nikolajsen, R. P., Mogensen, K. B., Kutter, J. P., *Electrophoresis* 2004, *25*, 253–269.

[67] Xuan, X., Li, D., *Electrophoresis* 2005, *26*, 166–175.

[68] Gaš, B., Kenndler, E., *Electrophoresis* 2000, *21*, 3888–3897.

[69] Gaš, B., Kenndler, E., *Electrophoresis* 2002, *23*, 3817–3826.

[70] Tang, G., Yang, C., Chai, C. K., Gong, H. Q., *Int. J. Heat Mass Trans.* 2004, *47*, 215–227.

[71] Tang, G., Yang, C., Chai, C. K., Gong, H. Q., *Anal. Chim. Acta* 2004, *507*, 27–37.

[72] Tang, G., Yang, C., Chai, C. K., Gong, H. Q., *Langmuir* 2003, *19*, 10975–10984.

[73] Xuan, X., Xu, B., Sinton, D., Li, D., *Lab Chip* 2004, *4*, 230–236.

[74] Tang, G., Yan, D., Yang, C., Gong, H. Q. *et al.*, *Electrophoresis* 2006, *27*, 628–639.

[75] Johnson, T. J., Ross, D., Gaitan, M., Locascio, L. E., *Anal. Chem.* 2001, *73*, 3656–3661.

[76] Xuan, X., Li, D., *J. Chromatogr. A* 2005, *1064*, 227–237.

[77] Chein, R., Yang, Y. C., Lin, Y., *Electrophoresis* 2006, *27*, 640–649.

[78] Tang, G., Yang, C., Gong, H. Q., Chai, C. *et al.*, *J. Heat Trans.* 2005, *127*, 660–663.

[79] Tang, G., Yang, C., Gong, H. Q., Chai, C. *et al.*, *Anal. Chim. Acta* 2006, *561*, 138–149.

[80] Xuan, X., Hu, G., Li, D., *Electrophoresis* 2006, *27*, 3171–3180.

[81] Barthe, L., Ribet, J., Pelissou, M., Degude, M. *et al.*, *J. Chromatogr. A* 2002, *968*, 241–250.

[82] Bean, S. R., Tilley, M., *Cereal Chem.* 2003, *80*, 505–510.

[83] Sowell, J., Parihar, G., Patonay, G., *J. Chromatogr. B* 2001, *752*, 1–8.

[84] Zhao, T., Liao, Q., *J. Micromech. Microeng.* 2002, *12*, 962–970.

[85] Maynes, D., Webb, B. W., *Int. J. Heat Mass Trans.* 2003, *46*, 1359–1369.

[86] Horiuchi, K., Dutta, P., *Int. J. Heat Mass Trans.* 2004, *47*, 3085–3095.

[87] Rathore, A. S., Reynolds, K. J., Colon, L. A., *Electrophoresis* 2002, *23*, 2918–2928.

[88] Chen, G., Tallerek, U., Seidel-Morgenstern, A., Zhang, Y., *J. Chromatogr. A* 2004, *1044*, 287–294.

[89] Kang, Y., Yang, C., Huang, X., *Langmuir* 2005, *21*, 7598–7607.

[90] Chang, M. H., Homsy, G. M., *Phys. Fluids* 2005, *17*, 074107.

[91] Wang, Y., Lin, Q., Mukherjee, T., *Lab Chip* 2004, *4*, 625–631.

[92] Evenhuis, C. J., Guijt, R. M., Macka, M., Marriott, P. J., Haddad, P. R., *Electrophoresis* 2005, *26*, 4333–4344.

[93] Evenhuis, C. J., Guijt, R. M., Macka, M., Marriott, P. J., Haddad, P. R., *Anal. Chem.* 2006, *78*, 2684–2693.

[94] Xuan, X., *Electrophoresis* 2007, *28*, 2971–2974.

[95] Hildreth, D., *J. Phys. Chem.* 1970, *74*, 2006–2015.

[96] Erickson, D., Sinton, D., Li, D., *Lab Chip* 2003, *3*, 141–149.

[97] Lim, D. S. W., Kuo, J. S., Chiu, D. T., *J. Chromatogr. A* 2004, *1027*, 237–244.

[98] Huang, K. D., Yang, R. J., *Electrophoresis* 2006, *27*, 1957–1966.

[99] Hu, G., Xiang, Q., Fu, R., Xu, B., Venditti, R., Li, D., *Anal. Chim. Acta* 2006, *557*, 146–151.

[100] Pawliszyn, J., Wu, J., *J. Microcol. Sep.* 1993, *5*, 397–401.

[101] Fang, X., Adams, M., Pawliszyn, J., *Analyst* 1999, *124*, 335–341.

[102] Huang, T., Pawliszyn, J., *Electrophoresis* 2002, *23*, 3504–3510.

[103] Huber, D., Santiago, J. G., *J. Heat Trans.* 2005, *127*, 806–806.

[104] Shackman, J. G., Munson, M. S., Ross, D., *Anal. Bioanal. Chem.* 2007, *387*, 155–158.

[105] Kim, S. M., Sommer, G. J., Burns, M. A., Hasselbrink, E. F., *Anal. Chem.* 2006, *78*, 8028–8035.

[106] Sigurdson, M., Wang, D. Z., Meinhart, C. D., *Lab Chip* 2005, *5*, 1366–1373.

[107] Morgan, H., Green, N. G., *AC Electrokinetics: Colloids and Nanoparticles*, Research Studies Press Ltd., Baldock, Hertfordshire, England 2003.

[108] Wang, D., Sigurdson, M., Meinhart, C. D., *Exp. Fluid* 2005, *38*, 1–10.

[109] Ramos, A., Morgan, H., Green, N. G., Castellanos, A., *J. Phys. D: Appl. Phys.* 1998, *31*, 2338–2353.

[110] Tang, S., Mayers, B. T., Vezenov, D. V., Whitesides, G. M., *Appl. Phys. Lett.* 2006, *88*, 061112.

[111] Chen, C. H., Lin, H., Lele, S. K., Santiago, J. G., *J. Fluid Mech.* 2005, *524*, 263–303.

